



Thermal oxidation aging of polydicyclopentadiene and composites

Yinghui Hu*, Yunpeng Zhang, Steven Nutt

M.C. Gill Composites Center, Department of Chemical Engineering and Materials Science, University of Southern California, Los Angeles, California

* E-mail: yinghuih@usc.edu

Abstract: The thermal aging and oxidation behavior of polydicyclopentadiene and composites was investigated, and the effects on thermal and mechanical properties were determined. Thermal and mechanical properties were measured by dynamic mechanical analysis, static tensile test, and short-beam shear tests. Diffusion limited oxidation was observed and oxidation was limited within the surface region ($\sim 100 \mu\text{m}$) of the sample. Single-fiber push-out test methodology was developed to directly measure the bond strength of fiber-matrix interface, and results showed that aging of composites at 150°C caused significant degradation of the fiber-matrix interface, while aging at 100°C for up to half a year had little effect on interface properties. The fiber-matrix interface strength near exposed surfaces decreased more quickly during aging compared to nonoxidized regions far beneath surfaces. POLYM. COMPOS., 2016. © 2016 Society of Plastics Engineers

1. INTRODUCTION

In recent years, polymer composites are used increasingly in civil applications, including wind turbine blades, offshore oil platforms, and oil and gas pipelines. For the protective shell of oil pipelines, temperatures can reach 80°C . Thus, long-term thermal aging and oxidation behavior is a major concern because these components are required to last decades with minimal maintenance [1-10]. Compared to traditional polymers, polydicyclopentadiene (pDCPD) has shown superior

Y. Hu, Y. Zhang, and S.R. Nutt, "Thermal oxidation aging of polydicyclopentadiene and composites" Polymer Composites, in press June (2016) DOI: [10.1002/pc.24125](https://doi.org/10.1002/pc.24125)



corrosion resistance in hygrothermal environments [11, 12] and is thus a natural candidate matrix for composites intended for severe service environments. However, the aging behavior of pDCPD in thermal oxidizing environments has not been systematically studied. Richaud et al. [13] studied the thermo-oxidative aging behavior of thin-film (20 μm) unstabilized pDCPD in glassy state, revealing that the specific formulation of the pDCPD studied showed faster oxidation rates than common polymers (e.g. polydienic elastomers) because of the high initiation rate and low termination rate during oxidation. To date, no systematic investigation of the thermo-oxidative aging of bulk pDCPD resin and composites has been reported. The present study addresses this topic, because structures in practical applications generally exist in bulk form rather than in thin films. The chemical reactions that occur in polymers during thermal-oxidative aging include postcuring, secondary polymerization, carbonyl growth, chain scission, volatile release, and oxidation [14]. Oxidation and diffusion also can affect mechanical behavior, and even small amounts of oxidation can significantly change mechanical properties because of chain scission.

Some researchers have pointed out that two competing mechanisms operate during thermal oxidation [15]. One of these mechanisms is cross-linking or secondary polymerization activated by the high temperature. The additional cross-linking increases molecular weight, thereby increasing strength and T_g . This mechanism occurs throughout the thickness of the sample because it is a thermal effect. Competing with this mechanism, the chain-scission reaction results in molecular weight decrease, chain mobility increase, and T_g decrease. Oxidation can cause both cross-linking (especially when double bonds are present in the backbone) and chain-scission [16].

For many polymers, however, the oxidation reaction is limited to a thin surface layer because of diffusion-limited oxidation (DLO). The DLO effect arises when the oxygen consumption rate exceeds the oxygen diffusion rate of the polymer. Thus, the thickness of the



oxidation layer is determined by the ratio of the oxidation reaction rate to the oxygen diffusion rate. Many polymers exhibit low O₂ permeability, and thus oxidation results in a surface oxidized layer. The oxidized layer prevents or inhibits further oxygen diffusion into the material and acts as a protective shell if the oxidized material is solid and dense. The thickness of the oxidized layer (TOL) strongly depends on temperature since the oxidation is diffusion-controlled. However, mode I cracks can arise in the oxidized layer because of shrinkage relative to the bulk material.

The oxidation behavior of composites differs from that of neat resins and generally is more complex. If the interface bond between fibers and matrix is degraded, the fiber-matrix interfaces can provide pathways for accelerated diffusion of reacting species. Also, because of oxidation-induced matrix shrinkage and the different thermal expansion coefficients of fibers and matrices, stress concentration occurs at fiber-matrix interfaces, facilitating interface debonding [17-21]. Matrix-rich regions experience greater stress concentrations because of the greater shrinkage, and matrix shrinkage generally increases with conditioning time and oxygen pressure.

In unidirectional (UD) composites, the oxidation behavior differs in transverse and longitudinal directions [21]. In the transverse direction, if the fiber volume fraction is sufficiently low that fibers are rarely in mutual contact, the oxidation behavior resembles that of the neat resin, and oxidation is confined to a thin surface layer. However, the transverse diffusion rate in the composite is generally slower than that of the neat resin because fibers hinder oxygen diffusion [22, 23]. If, on the other hand, the fiber volume fraction is high and fibers are in mutual contact, fiber-matrix interfaces become pathways for accelerated diffusion of oxygen because the interfaces form a connected network, often leading to debonding. Considering oxidation in the longitudinal direction, UD composites can show significantly different aging behavior because interfaces



provide continuous pathways for accelerated diffusion, which can be further accelerated by the occurrence of oxidation-induced debonding.

This study is the third report of a series of studies addressing the environmental aging of a new formulation of pDCPD polymer (see Refs. [11] and [12]). In this study, the thermal aging behavior of thick samples of pDCPD polymer and pDCPD/glass fiber composites was investigated as a function of temperature and environment. The thermal and mechanical properties were monitored by dynamic mechanical analysis (DMA), static tensile tests, short-beam shear tests, and microscopic inspection. The effect of thermo-oxidative aging on the fiber-matrix interface strength was measured using a single fiber push-out method. There are no previous reports of this type of study. The mechanical properties of pDCPD composites are retained after aging below or above the glass transition temperature, although the fiber-matrix interface glass fiber composites is damaged during high-temperature aging. Oxidation is limited to a thin surface layer, which is typical of DLO behavior.

2. EXPERIMENTS

2.1. Sample Preparation

Samples of pDCPD (Proxima, Materia) neat resin and glass fiber composites were prepared to study effects of thermal aging. Neat resin panels were cured for 2 hr at 30°C, then postcured for 30 min at 100°C. Two sizes of panels were prepared: 8 mm thick panels were used for the surface aging study, while 4 mm thick panels were later cut into dogbone tensile specimens (ASTM D638 type I). UD glass fiber laminates were produced by vacuum infusion (Materia). Noncrimp fabric (E-LT 3500, Vectorply) comprised of E-glass (94 wt% PPG Hybon® 2026 in the warp direction and 6 wt% PPG Hybon® 2002 in the weft direction) was used, and the fiber volume fraction was



~58% (determined by burn-out). Two sizes of composite laminates were prepared: 2-ply (1.6 mm thick) laminates were used for 0° tensile testing, while 4-ply (3.2 mm thick) laminates were used for 90° testing and shear testing. In the UD laminates, 0° samples were loaded along the fiber direction, while 90° samples were loaded perpendicular to the fiber direction. Tables 1 and 2 show the basic properties of cured pDCPD and the glass fibers, respectively.

Table 1. Properties of cured pDCPD resin.

T _g	Density	Tensile modulus	Ultimate tensile strength	Tensile elongation
(°C)	(kg/m ³)	(GPa)	(MPa)	
124	1050	3.1	73	2.7%

Table 2. Properties of glass fiber.

Modulus (GPa)	Tensile strength (MPa)	Average fiber diameter (μm)
82.7	2790	17

2.2. Aging Conditions

Three aging conditions were used: 100°C in nitrogen, 100°C in air, and 150°C in air. These two temperatures were selected to determine the aging effects below and above T_g (the T_g of unaged pDCPD is ~130°C). Note that these aging temperatures are relatively high compared to the common operating temperature of oil pipelines (<80°C). A nitrogen aging environment was used to compare the aging effects with and without oxygen. Samples were aged in air using air-circulated temperature-controlled ovens, while samples aged in nitrogen were sealed in glass containers and placed in temperature-controlled ovens. The volume of the glass jar is 1 L and the total volume of samples inside is ~50 cm³, so the volume ratio of nitrogen to sample is about 20:1. The seal between the glass jar and the cover is a rubber ring and slight leakage of air into the glass containers is expected because of the sealing technique. The weight change of neat resin and composite samples were monitored using specific groups of 8 mm neat resin blocks and 4-ply



laminate blocks. The total aging period was 25 weeks, while a group of samples was removed from ovens at 0, 1, 4, 9, 16, and 25 weeks to measure and thermal and mechanical properties.

2.3. Dynamic Mechanical Analysis

DMA (Q800, TA Instruments) was conducted on neat resin samples to track the evolution of thermal properties. Single cantilever beam samples ($35 \times 12 \times 3$ mm, *length* \times *width* \times *thickness*) were cut from the center of the 8 mm thick resin block, avoiding possible effects of the aged surface layer. In accordance with ASTM D7028 [24], the test temperature was ramped from 50°C to 180°C at 5°C/min. Samples were tested in bending mode. Displacement control was used with a maximum strain of 0.1% and a loading frequency of 1 Hz. Time, temperature, storage modulus, loss modulus, and $\tan(\delta)$ were recorded during the test.

2.4. Microstructure

Color changes in the aged surface layer were observed microscopically (Keyence VHS). The 8 mm neat resin block was cut ($10 \times 10 \times 8$ mm) and the sample was mounted and polished to observe the surface layers in cross-section.

2.5. Static Tension

Static tensile tests were conducted on both neat resin and composite samples using standard protocols (ASTM D638 [25] for neat pDCPD and ASTM D3039 [26] for composites). The neat resin sample was a dog-bone coupon $60 \times 10 \times 4$ mm (*gauge length* \times *width* \times *thickness*). The 0° composite sample was $203 \times 23 \times 1.6$ mm (*gauge length* \times *width* \times *thickness*), while the 90° composite sample dimension was $203 \times 23 \times 3.2$ mm (*gauge length* \times *width* \times *thickness*). Both types of composite samples were tabbed at the gripping ends using fiberglass tabs to prevent premature failure. The loading rates for neat resin and composite samples were 5 and 2 mm/min,



respectively. Tensile strain data were recorded using an extensometer (Instron 2630-109) until sample rupture occurred. Load, time, displacement, and strain were recorded during tests. pDCPD samples and 90° composite samples were tested on a tabletop load frame (Instron 5567), while tests of 0° composite samples were conducted on a larger load frame (Instron 5585H).

2.6. Short-Beam Shear

Short-beam shear (SBS) tests are used to measure the interlaminar shear strength of composite laminates because samples generally fail by interlaminar shear in such tests. In accordance with ASTM D2344 [27], a 4-ply composite sample was used and the dimensions of SBS samples were $19.2 \times 6.4 \times 3.2$ mm (*length* \times *width* \times *thickness*). The fiber direction was oriented along the length. Samples were loaded in a three-point bend fixture at a rate of 1 mm/min using a span length of 12.8 mm, and tests were continued until the first load drop occurred. Load, time, and displacement were recorded, and the load at the first load drop was used to calculate the short-beam strength (SBS).

2.7. Fiber Push-Out

The single-fiber push-out test provides a direct method to measure fiber-matrix interface strength [28-31]. To prepare samples for the test, thin polished transverse sections are prepared from UD fiber composites. Individual fibers are pushed through the section using a flat-bottomed diamond tip while monitoring load and displacement. Figure 1 shows the interface debonding moment during the push-out process. The apparent interface shear strength τ_{app} is calculated from the following equation:

$$\tau_{app} = \frac{F}{\pi DL} \quad (1)$$



where F is the push-out failure load, D is the fiber diameter, and L is the fiber length (i.e., sample thickness).

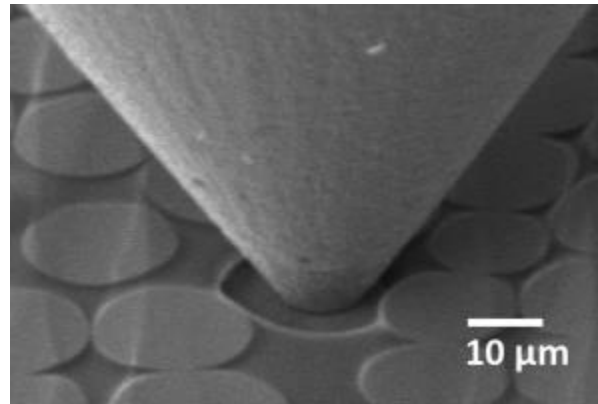


Figure 1. Fiber push-out test on glass/pDCPD composite.

The fiber push-out apparatus is integrated in a scanning electron microscope (SEM, JEOL JSM-6610LV) to leverage the imaging capabilities for positioning fibers beneath the tip. The push-out apparatus consists of a diamond tip (Hysitron, 10 μm tip diameter), a load sensor (Honeywell FSG020, range ± 5 N, resolution 0.4 mN), a drive motor (McLellan, resolution of 0.25 μm), a sample support, and computer control and data collection (LabView, National Instruments). An aluminum SEM specimen mount is used as the sample support and the sample is bonded to the support to prevent sliding during test. The specimen platform is machined with shallow grooves (0.5 mm wide) so that fibers can be pushed through without blockage. To prepare thin sections, both sides are polished to ~ 1 μm abrasive grit. The diameter of each pushed-out fiber is measured from SEM images.



3. RESULTS AND DISCUSSION

3.1. Weight Change

Figure 2 shows the weight change of neat resin and composite samples during thermal aging. The weight monitoring samples were the same as those used for DMA testing. Five samples were measured for each data point, and the maximum standard deviation was within 5% during the 25 weeks of aging. For samples aged in air at 100°C, the weight monotonically increased over 25 weeks of aging.

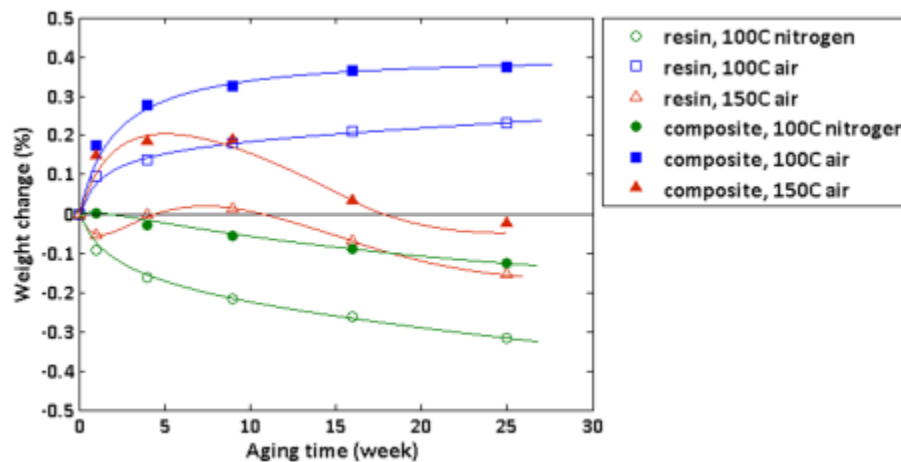


Figure 2. Weight change of samples. [Color figure can be viewed in the online issue, which is available at wileyonlinelibrary.com.]

The observed weight increases are attributed to surface oxidation, which produced an oxidized layer and increased sample weight [13, 32]. In contrast, samples aged in nitrogen at 100°C showed a monotonic decrease in weight during aging for 25 weeks. The weight loss is attributed to volatile molecules diffusing out from the samples (oxidation does not occur in the nitrogen ambient).

When samples were aged in air at 150°C, both oxidation and volatile diffusion were significant, causing simultaneous weight gain and weight loss. The oxidation reaction was relatively fast and short-term (because of passivation), while volatile diffusion was more



significant at longer aging times. This phenomenon is consistent with prior studies on similar CF/bismaleimide composites [4], where composite samples undergoing thermo-oxidative aging first showed a slight increase in weight followed by significant weight loss. Significant weight loss during aging at temperatures near or above T_g is common for most polymers [21, 33, 34].

Figure 2 also shows oxidation behavior for the neat resin, which can be compared to the oxidation behavior of composite samples. In general, composite samples showed greater weight gain (less weight loss) compared to neat resin samples. Glass fibers are inert to oxidation, and thus changes occur only in the matrix. The volume fraction of matrix in the composites was 40% (compared to 100% for the neat resin), and thus composite samples featured fewer volatile molecules per unit volume/weight. Oxidation, on the other hand, occurred by a surface reaction, and thus produced similar (%) weight gains in neat resin and composite samples. The net effect: composite samples showed less weight loss compared to the neat resin.

3.2. Dynamic Mechanical Analysis

Figure 3 shows the loss modulus curves after aging for 25 weeks under three aging conditions. The T_g of the un-aged pDCPD resin, determined from the loss modulus peak, is also marked on the plot ($\sim 130^\circ\text{C}$). After 9 weeks of aging, samples aged in air at 100°C show a slight decrease in T_g , while samples aged in nitrogen at 100°C show a greater decrease in T_g . The decreases are interpreted as a plasticization effect, whereby small molecules produced by chain scission during thermal aging act as plasticizers, decreasing the T_g . Samples aged in air show higher T_g values than those aged in nitrogen and showed surface discoloration from an oxidation layer. Likewise, samples aged in air at 150°C show a significant increase in T_g , although samples aged at 100°C did not. Secondary polymerization (postcuring) occurs at the higher aging temperature and leads to an increase in T_g .

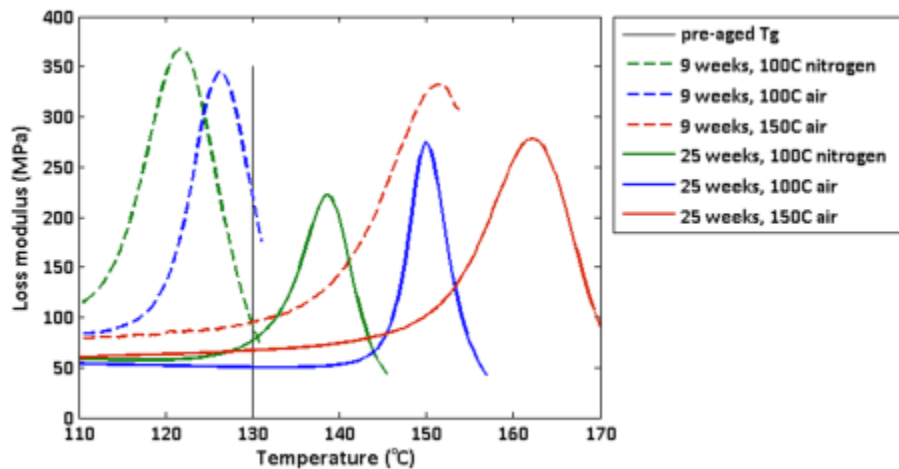


Figure 3. DMA curves of neat cured resin. [Color figure can be viewed in the online issue, which is available at wileyonlinelibrary.com.]

After 25 weeks of aging, samples aged in all three environments showed increases in T_g , a result caused by secondary polymerization during long-term thermal aging [35]. Among the three environments, aging in the 100°C nitrogen environment produced the lowest T_g (compared to 100°C air and 150°C air), a result attributed to the absence of an oxidized layer. Aging at higher temperatures in air led to more severe oxidation and thicker oxidation layers, causing higher overall T_g values for the whole sample.

3.3. Surface Aged Layer

Figure 4 shows the surface color change that arose during aging under different conditions. The surface oxidized layer for the 100°C air aged sample is marked in the enlarged insets. The dark surface layer results from oxidation (referred to as an oxidized layer) and is limited to the surface region of the sample—a clear DLO effect. The TOL is an important property for thermal aging of polymers and the TOL evolution versus aging time is plotted in Figure 5. Five samples were measured per data point, and the maximum standard deviation was less than 8%. The TOL approaches a saturated value after long-term aging, a result of a faster oxygen consumption rate compared to the oxygen diffusion rate.

Y. Hu, Y. Zhang, and S.R. Nutt, “Thermal oxidation aging of polydicyclopentadiene and composites” *Polymer Composites*, in press June (2016) DOI: [10.1002/pc.24125](https://doi.org/10.1002/pc.24125)

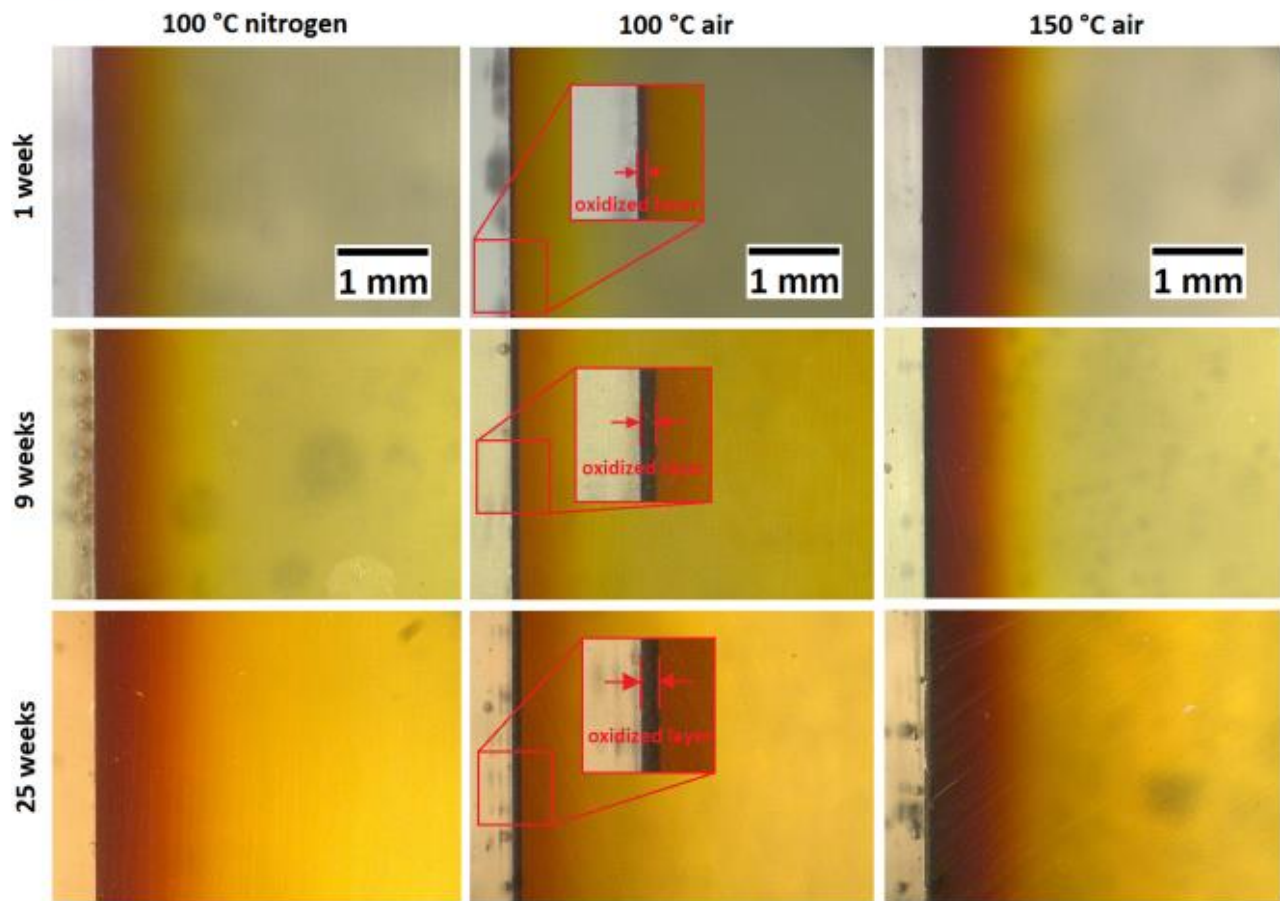


Figure 4. Polished sections of samples aged in different environments. [Color figure can be viewed in the online issue, which is available at wileyonlinelibrary.com.]

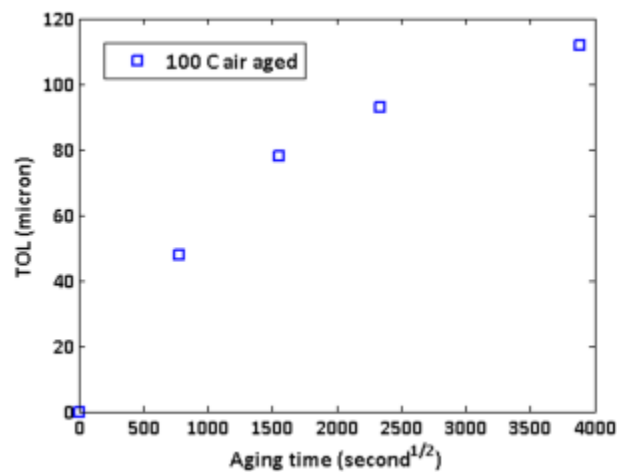


Figure 5. Thickness of oxidized layer (100°C air). [Color figure can be viewed in the online issue, which is available at wileyonlinelibrary.com.]



Others have reported TOL values of different polymers under different aging conditions. For example, Colin et al. [4] reported the TOL of CF/bismaleimide UD composite as $\sim 80 \mu\text{m}$ after 200 hr of aging, measured from modulus profile. Gigliotti et al. [19] found that the TOL of CF/epoxy composite was $\sim 200 \mu\text{m}$ after 430 hr of aging in 150°C air, while Yang et al. [32] reported TOL of $60\text{--}100 \mu\text{m}$ of anhydride-cured epoxy after 1 month aging in 160°C air, measured from DMA profile. Fan et al. [33] measured the TOL of CF/epoxy composite as 0.86 mm after 1200 hr of aging in 140°C air (measured from color change), while Zhang et al. [36] reported a TOL plateau of 0.8 mm in CF/epoxy composite is reached after 16 days of aging in 180°C (above T_g) air. Thus, the TOL of pDCPD in this study is within the reported range of values, indicating that although the initial oxidation rate of pDCPD is high [13], the oxidized layer can retard and even arrest further oxidation into bulk material.

Figure 4 shows that the sample aged in air at 100°C exhibits a distinctive dark surface layer, while the sample aged in nitrogen at 100°C shows slight discoloration. The color change of samples aged in nitrogen arises from surface carbonization and diffusion of small molecules out through the surface at high temperature-oxidation is not involved. Zhang et al. [37] studied thermal aging of epoxy and found similar surface aging phenomenon. The TOL reached a saturation value of 0.8 mm after 15 days of aging, protecting the bulk material from further oxidation.

Figure 4 also shows that samples aged at 150°C show a greater degree of darkening and a broader region of color change compared to samples aged at 100°C . The thickness of oxidized layer is difficult to measure accurately because there is no discrete boundary. The total thickness of the discolored region is $\sim 2 \text{ mm}$ because the DLO above T_g is less pronounced because of modification of the termination process of oxidation [13].



3.4. Static Tension

Figure 6 shows the evolution of tensile modulus and ultimate tensile strength (UTS) with aging time for 0° and 90° composites. Five samples were tested per data point, and the standard deviation bars are shown in Fig. 6. The maximum standard deviation in modulus for 0° samples was 12%, while for 90° samples, the deviation in modulus was 9%. The maximum standard deviation values for UTS of 0° and 90° samples was 9% and 17%, respectively. For 0° composites, the elastic modulus decreased 7% after 25 weeks of aging (compared to the un-aged condition). The elastic modulus after aging at 100°C and 150°C was unchanged. This result is consistent with previous studies. For example, Mourid et al. [34] reported that the modulus of CF/polyimide composite only decreased by 1% after 1 year aging near T_g . Similarly, Middleton et al. [38] studied the thermal aging of hybrid composite rod in 180°C (below T_g) air and reported modulus decrease by 15% after 1 year.

The 0° UTS after aging for 25 weeks at 100°C decreases by 2%, while the UTS after aging at 150°C decreases by 13%. The retention of modulus values reflects the inertness of glass fibers to thermal aging, because the 0° composite modulus is fiber-dominated. The retention of UTS for aging in air at 100°C reflects the stability of fiber-matrix interfaces, while the 13% decrease in UTS after aging at 150°C indicates partial degradation of interfaces, because 0° UTS is affected by both fiber and interface. Previous studies have shown that thermal aging can significantly decrease the strength of composites. Haque et al. [21] reported that the bending strength of CF/bismaleimide laminate decreased by 95% after 3000 hr aging in air near T_g , and Mourid et al. [34] reported 30% drop in tensile strength of CF/polyimide composite after 1 year of aging near T_g . Zhang et al. [36] reported 10% decrease in compressive strength of CF/epoxy composite after 16 days of aging in 180°C air (above T_g). Middleton et al. [38] found that the bending strength of hybrid composite

Y. Hu, Y. Zhang, and S.R. Nutt, “**Thermal oxidation aging of polydicyclopentadiene and composites**” Polymer Composites, in press June (2016) DOI: [10.1002/pc.24125](https://doi.org/10.1002/pc.24125)



rod decreased by 25% after 1 year of aging in 180°C air (below T_g). Souza Rios et al. [39] studied the weathering of polyurethane/epoxy/fiberglass and reported a similar trend—the strength first decreased and then increased after 180 days of aging.

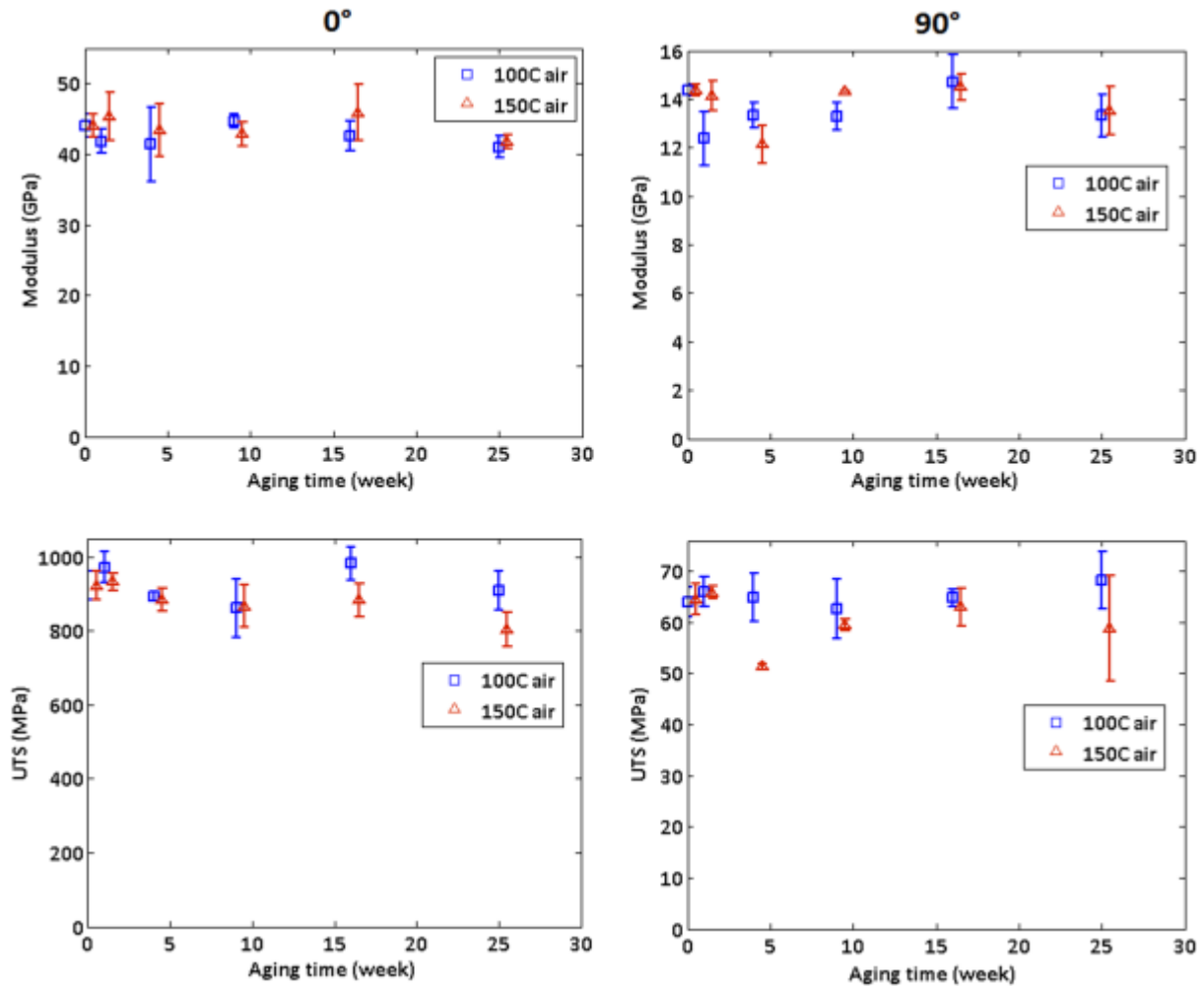


Figure 6. Tensile properties of 0° and 90° composites. [Color figure can be viewed in the online issue, which is available at wileyonlinelibrary.com.]

Figure 6 also shows the evolution of modulus and UTS for 90° composites, where mechanical properties typically depend strongly on both matrix and interfaces. The results reflect complex changes in matrix and interfaces. The moduli after aging for 25 weeks in air at 100°C and at 150°C show little difference (decrease by 4%). The negligible change in 90° modulus values reflects the



stability of the matrix modulus (the fiber modulus will not change during aging). The UTS of samples aged in air at 100°C shows a 7% increase, while aging at 150°C in air produced an 8% decrease after 25 weeks of aging. The negligible difference in UTS from the two aging conditions reflects concurrent reactions that produce matrix strengthening and interface degradation. During 100°C aging, interface strength is largely unchanged, while for 150°C aging, the interface is degraded. This conclusion is consistent with the analysis of aging effects on 0° composites.

Figure 7 shows stress-strain curves for 90° composites aged at 100°C and 150°C. Curves are artificially offset for clear display. After 16 weeks of aging in air, the 150°C sample shows early onset of plasticity (at ~25 MPa), while the sample aged at 100°C behaved similarly to the un-aged condition. The early plasticity of the composite aged at 150°C can be attributed either to the early plasticity of matrix, or to extensive debonding. Extensive interface debonding reportedly can cause macro-level plasticity during transverse tensile loading of UD composites [32]. Later evidence will show this to be the case. This early-stage plasticity causes the increased elongation at break after aging, which is contrary to commonly observed behavior (usually elongation of polymer composites will largely decrease after thermal aging) [13].

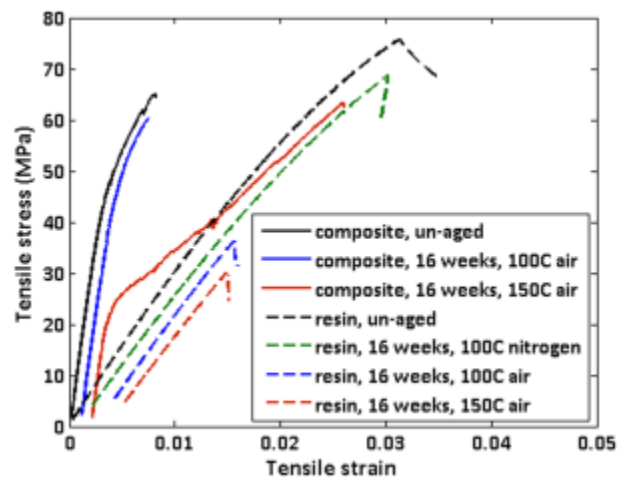


Figure 7. Stress-strain curves of neat resin and 90° composite. [Color figure can be viewed in the online issue, which is available at wileyonlinelibrary.com.]



Figure 7 also shows the evolution of stress-strain behavior for aged neat resin samples. After 16 weeks of aging, samples aged in air showed premature failure, while the modulus was unchanged, which is an indication of embrittlement. The embrittlement after aging in air is linked to surface oxidation, which resulted in a relatively brittle surface layer. Aging at 100°C and 150°C produced similar decreases in strength and failure strain, indicating similar degrees of surface aging. In contrast, the samples aged in nitrogen did not show embrittlement, and the strength and failure strain values were similar to those for the pre-aged condition.

Comparing the stress-strain curves of the neat resin and composites, the early plasticity of composites aged at 150°C was caused not by matrix degradation, but by interface degradation. This observation is consistent with previous discussion: aging at 150°C causes significant interface damage, while aging at 100°C does not.

Figure 8 shows the fracture surfaces of 90° tensile tested samples that had been aged for 1 week under different aging conditions. For the sample aged at 100°C, the fracture surface was dominated by matrix failure and no exposed fiber surface was observed, indicating retention of fiber-matrix bonding. In contrast, the fracture surface of the sample aged at 150°C consisted of substantial bare glass fiber resulting from interface debonding, indicating degraded fiber-matrix adhesion. The micrographs are consistent with the discussion of tensile properties (Figs. 6 and 7).

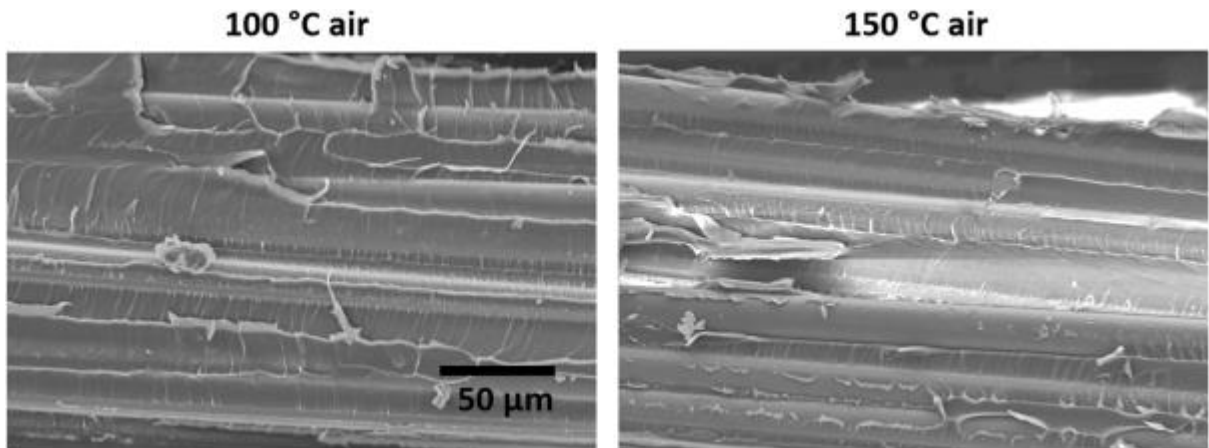


Figure 8. Fractography of 90° tensile after 1 week of aging.

3.5. Interface Strength

Figure 9 shows the evolution of interface strength (τ_{app}) as a function of aging time in air at 100°C and 150°C, as determined from fiber push-out tests. The aging times for all aging conditions are 0, 9, 16, and 25 weeks-adjacent data points are artificially offset for clarity. Each data point represents 15 valid tests, and the error bars represent standard deviations. The maximum standard deviation is 11% for “100°C air inside” interfaces, 11% for “100°C air surface” interfaces, and 23% for “150°C air inside” interfaces. Quantitative measurement of interface strength evolution during thermal aging has not been previously reported. However, there have been multiple observations of matrix shrinkage, matrix cracking and interface debonding during thermal aging [21, 22, 38], all of which indicate a detrimental effect.

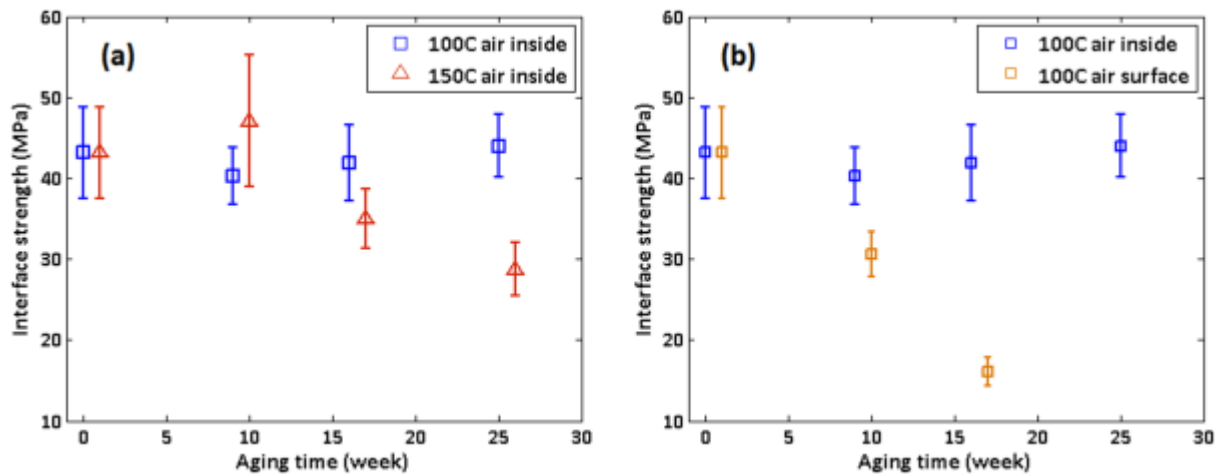


Figure 9. Interface strength from fiber push-out test (a) from fibers inside the samples of 100°C and 150°C air aged; (b) from fibers inside the samples and near the sample surface of 100°C air aged). [Color figure can be viewed in the online issue, which is available at wileyonlinelibrary.com.]

Figure 9a shows τ_{app} values for fibers situated far from the surface aged layer, which are thus less affected by oxidation. In contrast, Fig. 9b shows τ_{app} values for fibers situated near the surface, which highlight the adverse effects of oxidation on interface strength. Near-surface fibers for samples aged at 100°C and 150°C in air for 25 weeks could not be measured, because the embrittled surface layer was prohibitively fragile.

Figure 9a shows that no significant change in τ_{app} occurred after aging at 100°C in air, and the error bars from different aging times overlap. In contrast, after aging at 150°C in air for 16 weeks, the τ_{app} showed a slight decrease and continued to decrease after aging for 25 weeks. The value of τ_{app} after 25 weeks was 67% compared to the pre-aged condition, indicating significant damage to the interface as a result of thermal aging. The results shown in Figure 9a are consistent with the analysis of Figure 7, in which the early onset of plasticity after aging in air at 150°C was attributed to extensive interface debonding.



Figure 9b shows that the τ_{app} for near-surface fibers decreased substantially because of oxidation. The τ_{app} of near-surface fibers dropped to 37% after 16 weeks of aging in air, while the retention of τ_{app} of interior fibers was 97% for the same aging treatment. Clearly, high-temperature oxidation degraded interface strength more severely than high temperature aging alone. Thus, if the oxidation depth cannot be restricted, the mechanical properties of the composite will decrease significantly because of interface degradation and matrix embrittlement.

Figure 10 shows the evolution of short-beam strength with aging time. Five samples were tested per data point and the standard deviation bars are shown in Figure 10. The maximum standard deviation for samples aged both at 100°C and 150°C in air was 5%. Samples aged at 150°C showed greater decrease in SBS (20% after 16 weeks) compared to samples aged at 100°C (1% after 16 weeks). This behavior is consistent with the trend shown previously in Figure 10. The short-beam shear strength of composites reflects both matrix shear strength and interface shear strength. From the previous discussion, the observed decrease in SBS can be attributed to degradation of interface strength induced by thermal oxidation.

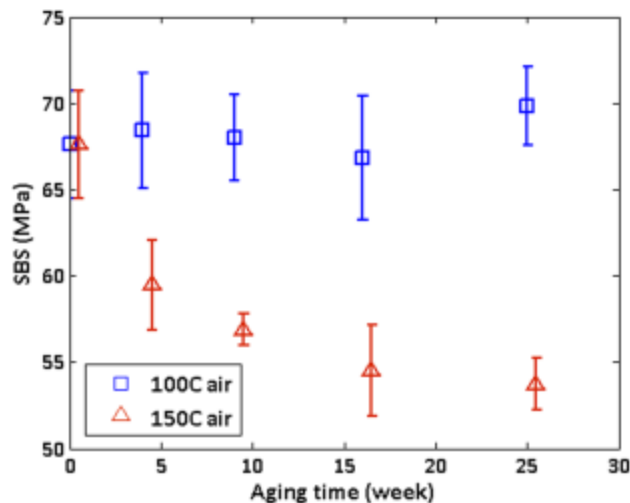


Figure 10. Short-beam strength degradation. [Color figure can be viewed in the online issue, which is available at wileyonlinelibrary.com.]



4. CONCLUSIONS

The thermal aging and oxidation behavior of thick samples of pDCPD polymer and UD glass fiber composites were investigated. DLO is observed for the pDCPD formulation studied, and oxidation is limited to a thin surface layer ($\sim 100 \mu\text{m}$) on the sample. The mechanical properties of the pDCPD neat resin and composites were stable for up to 25 weeks of aging, and the glass transition temperature increased after long-term thermal aging. High temperature aging of composites in air (150°C) caused significant damage to interfaces compared to low-temperature aging (100°C), as evidenced by 90° tensile tests. The interface strength decreased during aging, although the extent of degradation varied with subsurface depth, and degradation was most pronounced in near-surface regions. Thus, interface damage will be a concern in oxidative conditions, and protective coatings may be required in the most severe service environments.

Thermal aging of polymers and composites is a key issue for high-temperature applications, particularly in the oil and gas industry, where risers, casings, pipelines, and other components see hot/wet environments for protracted periods. The particular pDCPD formulation chosen for study is stable when exposed to the thermal aging environments selected here. The formulation is thus suitable for consideration for use in aggressive service environments and for substitutes for conventional metallic alloys, particularly in corrosive environments. The pDCPD resin also has appealing characteristics relative to conventional resins such as epoxy, including ultra-low viscosity, which facilitates infusion, and intrinsic hydrophobicity, which imparts superior moisture resistance. Further investigations of other types of aging and conditions (e.g., creep, microbiologically induced corrosion, high pressure) are required before deployment in actual service applications, and interactions between these factors must be understood to accurately predict longevity.

Y. Hu, Y. Zhang, and S.R. Nutt, “**Thermal oxidation aging of polydicyclopentadiene and composites**” *Polymer Composites*, in press June (2016) DOI: [10.1002/pc.24125](https://doi.org/10.1002/pc.24125)



Acknowledgements: The authors thank Rohan Dhall and Dr. Matthew Mecklenburg from Center for Electron Microscopy and Microanalysis (CEMMA) of University of Southern California and August Lang from USC Composites Center for building the prototype of the fiber push-out tester. The authors also acknowledge Patricio Martinez and Dr. Yuzheng Zhang of USC's M.C. Gill Composites Center for assistance with fiber push-out tests.

References:

1. A. Schieffer, J.F. Maire, and D. Leveque, *Compos. Sci. Technol.*, 62, (2002).
2. S.J. Park, M.K. Seo, and D.R. Lee, *Carbon*, 41, (2003).
3. B.F. Abu-Sharkh and H. Hamid, *Polym. Degrad. Stab.*, 85, (2004).
4. X. Colin and J. Verdu, *Compos. Sci. Technol.*, 65, (2005).
5. J. Guisandez, P. Tiemblo, and J. M. Gomez-Elvira, *Polym. Degrad. Stab.*, 87, (2005).
6. M. Zenkiewicz, M. Rauchfleisch, J. Czuprynska, J. Polanski, T. Karasiewicz, and W. Engelgard, *Appl. Surf. Sci.*, 253, (2007).
7. L. Olivier, N.Q. Ho, J.C. Grandidier, and M.C. Lafarie-Frenot, *Polym. Degrad. Stab.*, 93, (2008).
8. L. Olivier, C. Baudet, D. Bertheau, J.C. Grandidier, and M.C. Lafarie-Frenot, *Composites A*, 40, (2009).
9. M.C. Lafarie-Frenot, J.C. Grandidier, M. Gigliotti, L. Olivier, X. Colin, J. Verdu, and J. Cinquin, *Polym. Degrad. Stab.*, 95, (2010).
10. F. Awaja, M.T. Nguyen, S. Zhang, and B. Arhatari, *Composites A*, 42, (2011).
11. Y. Hu, A.W. Lang, X. Li, and S.R. Nutt, *Polym. Degrad. Stab.*, 110, (2014).
12. Y. Hu, X. Li, A.W. Lang, Y. Zhang, and S.R. Nutt, *Polym. Degrad. Stab.*, 124, (2016).
13. E. Richaud, P.Y. Le Gac, and J. Verdu, *Polym. Degrad. Stab.*, 102, (2014).
14. M.C. Celina, *Polym. Degrad. Stab.*, 98, (2013).
15. J. Middleton, B. Burks, T. Wells, A.M. Setters, I. Jasiuk, P. Predecki, J. Hoffman, and M. Kumosa, *Polym. Degrad. Stab.*, 98, (2013).
16. A. Boubakri, N. Guermazi, K. Elleuch, and H.F. Ayedi, *Mater. Sci. Eng. A*, 527, (2010).
17. M. Gigliotti, J.C. Grandidier, and M.C. Lafarie-Frenot, *Compos. Struct.*, 93, (2011).
18. M. Gigliotti, L. Olivier, D.Q. Vu, J.C. Grandidier, and M.C. Lafarie-Frenot, *J. Mech. Phys. Solids*, 59, (2011).
19. M. Gigliotti, J.C. Grandidier, and M.C. Lafarie-Frenot, *Mech. Mater.*, 43, (2011).
20. M. Gigliotti, Y. Pannier, M. Minervino, M.C. Lafarie-Frenot, and P. Corigliano, *Compos. Struct.*, 106, (2013).
21. M.H. Haque, P. Upadhyaya, S. Roy, T. Ware, W. Voit, and H. Lu, *Compos. Struct.*, 108, (2014).
22. D.Q. Vu, M. Gigliotti, and M.C. Lafarie-Frenot, *Composites A*, 43, (2012).
23. D.Q. Vu, M. Gigliotti, and M.C. Lafarie-Frenot, *Composites A*, 44, (2013).



24. Standard Test Method for Glass Transition Temperature (DMA T_g) of Polymer Matrix Composites by Dynamic Mechanical Analysis (DMA), Designation: D 7028 – 07, ASTM International.
25. Standard Test Method for Tensile Properties of Plastics, Designation: D638 – 10, ASTM International.
26. Standard Test Method for Tensile Properties of Polymer Matrix Composite Materials, Designation: D3039/D3039M – 08, ASTM International.
27. Standard Test Method for Short-Beam Strength of Polymer Matrix Composite Materials and Their Laminates, Designation: D2344/D2344M – 00 (Reapproved 2006), ASTM International.
28. X.F. Zhou, H.D. Wagner, and S.R. Nutt, *Composites A*, 32, (2001).
29. G.P. Tandon and N.J. Pagano, *Compos. Sci. Technol.*, 58, (1998).
30. M. Greisel, J. Jager, J. Moosburger-Will, M.G.R. Sause, W.M. Mueller, and S. Horn, *Composites A*, 66, (2014).
31. S.S. Rangaraj and S.B. Bhaduri, *J. Mater. Sci.*, 29, (1994).
32. Y. Yang, G. Xian, H. Li, and L. Sui, *Polym. Degrad. Stab.*, 118, (2015).
33. W. Fan, J. Li, Y. Zheng, T. Liu, X. Tian, and R. Sun, *Polym. Degrad. Stab.*, 123, (2016).
34. A. El Mourid, R. Ganesan, M. Brochu, T. Crochon, and M. Levesque, *Composites B*, 76, (2015).
35. Y. Hu, N.K. Kar, and S.R. Nutt, *Polym. Compos.*, 36, (2015).
36. M. Zhang, C. Zuo, B. Sun, and B. Gu, *Compos. Struct.*, 140, (2016).
37. M. Zhang, B. Sun, and B. Gu, *Composites A*, 85, (2016).
38. J. Middleton, J. Hoffman, B. Burks, P. Predecki, and M. Kumosa, *Composites A*, 69, (2015).
39. A. Souza Rios, W.F. Amorim Júnior, E.P. Moura, E.P. Deus, and J.P. Andrade Feitosa, *Polym. Test.*, 50, (2016).